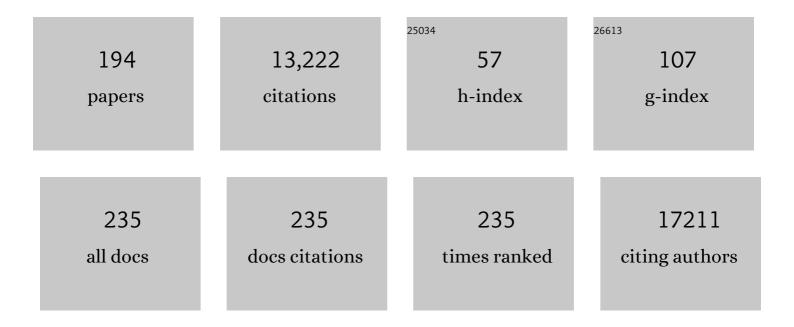
Paul A Bates

List of Publications by Year in descending order

Source: https://exaly.com/author-pdf/7478206/publications.pdf Version: 2024-02-01



#	Article	IF	CITATIONS
1	Genomic architecture and evolution of clear cell renal cell carcinomas defined by multiregion sequencing. Nature Genetics, 2014, 46, 225-233.	21.4	1,103
2	Enhancement of protein modeling by human intervention in applying the automatic programs 3D-JIGSAW and 3D-PSSM. Proteins: Structure, Function and Bioinformatics, 2001, 45, 39-46.	2.6	504
3	Global topological features of cancer proteins in the human interactome. Bioinformatics, 2006, 22, 2291-2297.	4.1	458
4	Structure of the AAA ATPase p97. Molecular Cell, 2000, 6, 1473-1484.	9.7	394
5	Reversal of DNA alkylation damage by two human dioxygenases. Proceedings of the National Academy of Sciences of the United States of America, 2002, 99, 16660-16665.	7.1	357
6	Updates to the Integrated Protein–Protein Interaction Benchmarks: Docking Benchmark Version 5 and Affinity Benchmark Version 2. Journal of Molecular Biology, 2015, 427, 3031-3041.	4.2	348
7	Matrix geometry determines optimal cancer cell migration strategy and modulates response to interventions. Nature Cell Biology, 2013, 15, 751-762.	10.3	282
8	The binding site on ICAM-1 for plasmodium falciparum-infected erythrocytes overlaps, but is distinct from, the LFA-1-binding site. Cell, 1992, 68, 71-81.	28.9	277
9	Repair of alkylated DNA: Recent advances. DNA Repair, 2007, 6, 429-442.	2.8	262
10	SwarmDock: a server for flexible protein–protein docking. Bioinformatics, 2013, 29, 807-809.	4.1	259
11	A structureâ€based benchmark for protein–protein binding affinity. Protein Science, 2011, 20, 482-491.	7.6	252
12	Agent-based simulation of notch-mediated tip cell selection in angiogenic sprout initialisation. Journal of Theoretical Biology, 2008, 250, 25-36.	1.7	234
13	Structure of an XRCC1 BRCT domain: a new protein-protein interaction module. EMBO Journal, 1998, 17, 6404-6411.	7.8	223
14	Planar polarization of the atypical myosin Dachs orients cell divisions in <i>Drosophila</i> . Genes and Development, 2011, 25, 131-136.	5.9	205
15	Recognition of analogous and homologous protein folds: analysis of sequence and structure conservation 1 1Edited by F. E. Cohen. Journal of Molecular Biology, 1997, 269, 423-439.	4.2	204
16	An automated classification of the structure of protein loops. Journal of Molecular Biology, 1997, 266, 814-830.	4.2	189
17	Tipping the Balance: Robustness of Tip Cell Selection, Migration and Fusion in Angiogenesis. PLoS Computational Biology, 2009, 5, e1000549.	3.2	187
18	OPCML at 11q25 is epigenetically inactivated and has tumor-suppressor function in epithelial ovarian cancer. Nature Genetics, 2003, 34, 337-343.	21.4	169

#	Article	IF	CITATIONS
19	Mathematical modeling identifies Smad nucleocytoplasmic shuttling as a dynamic signal-interpreting system. Proceedings of the National Academy of Sciences of the United States of America, 2008, 105, 6608-6613.	7.1	168
20	Butyrophilin-2A1 Directly Binds Germline-Encoded Regions of the Vγ9Vδ2 TCR and Is Essential for Phosphoantigen Sensing. Immunity, 2020, 52, 487-498.e6.	14.3	164
21	The γÎTCR combines innate immunity with adaptive immunity by utilizing spatially distinct regions for agonist selection and antigen responsiveness. Nature Immunology, 2018, 19, 1352-1365.	14.5	163
22	The Relationship between the Flexibility of Proteins and their Conformational States on Forming Protein–Protein Complexes with an Application to Protein–Protein Docking. Journal of Molecular Biology, 2005, 347, 1077-1101.	4.2	159
23	STRIPAK components determine mode of cancer cell migration and metastasis. Nature Cell Biology, 2015, 17, 68-80.	10.3	158
24	SwarmDock and the Use of Normal Modes in Protein-Protein Docking. International Journal of Molecular Sciences, 2010, 11, 3623-3648.	4.1	154
25	Cluster analysis of networks generated through homology: automatic identification of important protein communities involved in cancer metastasis. BMC Bioinformatics, 2006, 7, 2.	2.6	148
26	Prediction of homoprotein and heteroprotein complexes by protein docking and templateâ€based modeling: A CASPâ€CAPRI experiment. Proteins: Structure, Function and Bioinformatics, 2016, 84, 323-348.	2.6	148
27	SETD2 loss-of-function promotes renal cancer branched evolution through replication stress and impaired DNA repair. Oncogene, 2015, 34, 5699-5708.	5.9	147
28	Systematic Evaluation of the Prognostic Impact and Intratumour Heterogeneity of Clear Cell Renal Cell Carcinoma Biomarkers. European Urology, 2014, 66, 936-948.	1.9	141
29	Model building by comparison at CASP3: Using expert knowledge and computer automation. Proteins: Structure, Function and Bioinformatics, 1999, 37, 47-54.	2.6	138
30	PECAM-1: Its Expression and Function as a Cell Adhesion Molecule on Hemopoietic and Endothelial Cells. Leukemia and Lymphoma, 1995, 17, 229-244.	1.3	134
31	Community-Wide Assessment of Protein-Interface Modeling Suggests Improvements to Design Methodology. Journal of Molecular Biology, 2011, 414, 289-302.	4.2	131
32	The BRCA1 C-terminal domain: structure and function. Mutation Research DNA Repair, 2000, 460, 319-332.	3.7	128
33	Rational engineering of L-asparaginase reveals importance of dual activity for cancer cell toxicity. Blood, 2011, 117, 1614-1621.	1.4	122
34	Protein Determinants for Specific Polysialylation of the Neural Cell Adhesion Molecule. Journal of Biological Chemistry, 1995, 270, 17171-17179.	3.4	115
35	Ctf4 Links DNA Replication with Sister Chromatid Cohesion Establishment by Recruiting the Chl1 Helicase to the Replisome. Molecular Cell, 2016, 63, 371-384.	9.7	113
36	Protein–protein binding affinity prediction on a diverse set of structures. Bioinformatics, 2011, 27, 3002-3009.	4.1	103

#	Article	IF	CITATIONS
37	Conserved Residues of Human XPG Protein Important for Nuclease Activity and Function in Nucleotide Excision Repair. Journal of Biological Chemistry, 1999, 274, 5637-5648.	3.4	100
38	Opposing effects of Elk-1 multisite phosphorylation shape its response to ERK activation. Science, 2016, 354, 233-237.	12.6	100
39	Blind prediction of homo―and heteroâ€protein complexes: The CASP13â€CAPRI experiment. Proteins: Structure, Function and Bioinformatics, 2019, 87, 1200-1221.	2.6	99
40	The scoring of poses in protein-protein docking: current capabilities and future directions. BMC Bioinformatics, 2013, 14, 286.	2.6	98
41	Genetic analysis of integrin function in man: LAD-1 and other syndromes. Matrix Biology, 2000, 19, 211-222.	3.6	94
42	Modeling protein association mechanisms and kinetics. Current Opinion in Structural Biology, 2013, 23, 887-893.	5.7	87
43	Community-wide evaluation of methods for predicting the effect of mutations on protein-protein interactions. Proteins: Structure, Function and Bioinformatics, 2013, 81, 1980-1987.	2.6	87
44	A simple biophysical model emulates budding yeast chromosome condensation. ELife, 2015, 4, e05565.	6.0	87
45	The I Domain of Integrin Leukocyte Function-associated Antigen-1 Is Involved in a Conformational Change Leading to High Affinity Binding to Ligand Intercellular Adhesion Molecule 1 (ICAM-1). Journal of Biological Chemistry, 1998, 273, 27396-27403.	3.4	84
46	Different Smad2 partners bind a common hydrophobic pocket in Smad2 via a defined proline-rich motif. EMBO Journal, 2002, 21, 145-156.	7.8	84
47	Extracellular matrix anisotropy is determined by TFAP2C-dependent regulation of cell collisions. Nature Materials, 2020, 19, 227-238.	27.5	82
48	Automated classification of antibody complementarity determining region 3 of the heavy chain (H3) loops into canonical forms and its application to protein structure prediction. Journal of Molecular Biology, 1998, 279, 1193-1210.	4.2	80
49	An siRNA screen identifies RSK1 as a key modulator of lung cancer metastasis. Oncogene, 2011, 30, 3513-3521.	5.9	78
50	A FIJI macro for quantifying pattern in extracellular matrix. Life Science Alliance, 2021, 4, e202000880.	2.8	75
51	Prediction of protein assemblies, the next frontier: The <scp>CASP14 APRI</scp> experiment. Proteins: Structure, Function and Bioinformatics, 2021, 89, 1800-1823.	2.6	73
52	Crystal structure at 1.95 å resolution of the breast tumour-specific antibody SM3 complexed with its peptide epitope reveals novel hypervariable loop recognition. Journal of Molecular Biology, 1998, 284, 713-728.	4.2	72
53	The crystal and molecular structure of dichloro-1,2-bis(diphenylphosphino)ethanedigold(I). Inorganica Chimica Acta, 1985, 98, 125-129.	2.4	71
54	A dyad of lymphoblastic lysosomal cysteine proteases degrades the antileukemic drug l-asparaginase. Journal of Clinical Investigation, 2009, 119, 1964-73.	8.2	69

#	Article	IF	CITATIONS
55	Development of synchronous VHL syndrome tumors reveals contingencies and constraints to tumor evolution. Genome Biology, 2014, 15, 433.	8.8	69
56	Analysis of the Binding Site on Intercellular Adhesion Molecule 3 for the Leukocyte Integrin Lymphocyte Function-associated Antigen 1. Journal of Biological Chemistry, 1995, 270, 877-884.	3.4	68
57	A new type of pyridine-2-thionato bridge: X-ray crystal structure of the complex [Re2(MepyS)2(CO)6] where MepyS is the 6-methylpyridine-2-thionato ligand. Polyhedron, 1988, 7, 1401-1403.	2.2	64
58	Rhodium(III) complexes with pyridine-2-thiol (pySH) and pyridine-2-thiolato (pyS) as the only ligands: crystal structures of mer-[Rh(pyS)3], [Rh(pyS)2(pySH)2]Cl·0.5H2O, and [Rh(pyS)3(pySH)]. Journal of the Chemical Society Dalton Transactions, 1988, , 227-233.	1.1	60
59	A predicted three-dimensional structure for the carcinoembryonic antigen (CEA). FEBS Letters, 1992, 301, 207-214.	2.8	60
60	BRCT Domain Interactions in the Heterodimeric DNA Repair Protein XRCC1â^'DNA Ligase III. Biochemistry, 2001, 40, 5906-5913.	2.5	59
61	Recognition of Phosphorylated-Smad2-Containing Complexes by a Novel Smad Interaction Motif. Molecular and Cellular Biology, 2004, 24, 1106-1121.	2.3	59
62	Detection and refinement of encounter complexes for protein–protein docking: Taking account of macromolecular crowding. Proteins: Structure, Function and Bioinformatics, 2010, 78, 3189-3196.	2.6	59
63	Can MM-PBSA calculations predict the specificities of protein kinase inhibitors?. Journal of Computational Chemistry, 2006, 27, 1990-2007.	3.3	55
64	Characterisation of the single copy trefoil peptides intestinal trefoil factor and pS2 and their ability to form covalent dimers. FEBS Letters, 1995, 357, 50-54.	2.8	54
65	Implicit flexibility in protein docking: Crossâ€docking and local refinement. Proteins: Structure, Function and Bioinformatics, 2007, 69, 750-757.	2.6	53
66	Model building by comparison at CASP3: Using expert knowledge and computer automation. Proteins: Structure, Function and Bioinformatics, 1999, 37, 47-54.	2.6	53
67	A tetrahedral complex of gold(I). The crystal and molecular structure of Au(Ph2PCH2CH2PPh2)2Cl·2H2O. Inorganica Chimica Acta, 1984, 81, 151-156.	2.4	52
68	Blind prediction of interfacial water positions in CAPRI. Proteins: Structure, Function and Bioinformatics, 2014, 82, 620-632.	2.6	50
69	Selection of metastasis competent subclones in the tumour interior. Nature Ecology and Evolution, 2021, 5, 1033-1045.	7.8	50
70	Macroscopic pKa Calculations for Fluorescein and Its Derivatives. Journal of Chemical Theory and Computation, 2006, 2, 1520-1529.	5.3	49
71	Kinetic Rate Constant Prediction Supports the Conformational Selection Mechanism of Protein Binding. PLoS Computational Biology, 2012, 8, e1002351.	3.2	48
72	β-Diketone interactions. Part 8. The hydrogen bonding of the enol tautomers of some 3-substituted pentane-2,4-diones. Journal of the Chemical Society Perkin Transactions II, 1989, , 527-533.	0.9	47

#	Article	IF	CITATIONS
73	The structure of 2,2-di-t-butyl-1,3,2-dioxa-, -oxathia-, and -dithia-stannolanes: a study by solution and solid state NMR and single crystal X-ray diffraction. Journal of Organometallic Chemistry, 1989, 363, 45-60.	1.8	46
74	Flexible relaxation of rigid-body docking solutions. Proteins: Structure, Function and Bioinformatics, 2007, 68, 159-169.	2.6	44
75	Electrophile-mediated cyclisations: regioselective synthesis of substituted cyclic nitrones and crystal structures of the nitrone cycloadducts. Journal of the Chemical Society Perkin Transactions 1, 1989, , 2415.	0.9	43
76	A region encompassing the FERM domain of Jak1 is necessary for binding to the cytokine receptor gp130. FEBS Letters, 2001, 505, 87-91.	2.8	43
77	Oxidative addition of 1,3-diynes at triosmium clusters with cleavage of the central carbon–carbon bond: X-ray crystal structure of [Os3(µ3,η2-C2Ph)(µ-C2Ph)(CO)9] derived from 1,4-diphenylbuta-1,3-diyne. Journal of the Chemical Society Chemical Communications, 1987, , 461-463.	2.0	41
78	In silico Protein Recombination: Enhancing Template and Sequence Alignment Selection for Comparative Protein Modelling. Journal of Molecular Biology, 2003, 328, 593-608.	4.2	39
79	Di- and tri-nuclear complexes of palladium(II) containing doubly- and triply-bridging pyridine-2-thionato (pyS) ligands: crystal structure of [Pd3(C6H4CH2NMe2)3(pyS)2][BF4]. Journal of the Chemical Society Dalton Transactions, 1988, , 2193.	1.1	38
80	Cephalotaxine analogs: stereospecific synthesis of spiro-fused 3-benzazepine and 1,3-benzodiazepine derivatives. Journal of Organic Chemistry, 1990, 55, 1261-1266.	3.2	37
81	Intermediates in the conversion of [Os3(CO)11(PRPh2)](R = Me or Ph) into [Os3(µ3-C6H4)(µ3–PR)(CO)9]: crystal and molecular structures of [Os3-(µ-H)(µ3-C6H4PMePh-o)(CO)9] and [Os3(µ3-C6H4PMe-o)(CO)10]. Journal of the Chemical Society Dalton Transactions, 1987, , 1529-1534.	1.1	36
82	The syntheses, structures, and stereodynamics of [3]ferrocenophane complexes. Journal of Organometallic Chemistry, 1989, 367, 275-289.	1.8	36
83	IRaPPA: information retrieval based integration of biophysical models for protein assembly selection. Bioinformatics, 2017, 33, 1806-1813.	4.1	36
84	Notes. [RhPd2(pyS)4(η3-C4H7)2][BF4]: synthesis and X-ray structure of a mixed-metal trinuclear complex containing two Âμ3-pyridine-2-thionato (pyS) ligands. Journal of the Chemical Society Dalton Transactions, 1988, , 235-238.	1.1	35
85	Understanding cancer mechanisms through network dynamics. Briefings in Functional Genomics, 2012, 11, 543-560.	2.7	35
86	β-Diketone interactions. Part 6. X-Ray molecular structure of 3-(4-methoxyphenyl)pentane-2,4-dione, a β-diketone enol tautomer with a very strong hydrogen bond. Journal of the Chemical Society Perkin Transactions 1, 1988, , 297-299.	0.9	33
87	Structure and Function of Intercellular Adhesion Molecule-1. Chemical Immunology and Allergy, 1991, 50, 98-115.	1.7	33
88	Functional Recycling of C2 Domains Throughout Evolution: A Comparative Study of Synaptotagmin, Protein Kinase C and Phospholipase C by Sequence, Structural and Modelling Approaches. Journal of Molecular Biology, 2003, 333, 621-639.	4.2	33
89	Preparation of niobium and tantalum organoimido complexes from reactions of the pentahalides with amines: The crystal and molecular structure of bis(t-butylamine)bis(t-butylimido)bis(μ-ethoxy)tetrachloroditantalum. Polyhedron, 1985, 4, 1391-1401.	2.2	32
90	A Markovâ€chain model description of binding funnels to enhance the ranking of docked solutions. Proteins: Structure, Function and Bioinformatics, 2013, 81, 2143-2149.	2.6	32

#	Article	IF	CITATIONS
91	Hydrogen bonding between free fluoride ions and water molecules: two X-ray structures. Journal of Molecular Structure, 1990, 220, 1-12.	3.6	31
92	β-diketone interactions. Journal of Molecular Structure, 1988, 178, 297-303.	3.6	30
93	Guided docking: First step to locate potential binding sites. Proteins: Structure, Function and Bioinformatics, 2003, 52, 28-32.	2.6	30
94	Spatial patterns of tumour growth impact clonal diversification in a computational model and the TRACERx Renal study. Nature Ecology and Evolution, 2022, 6, 88-102.	7.8	30
95	Novel use of a genetic algorithm for protein structure prediction: Searching template and sequence alignment space. Proteins: Structure, Function and Bioinformatics, 2003, 53, 424-429.	2.6	29
96	Incorporation of flexibility into rigid-body docking: Applications in rounds 3-5 of CAPRI. Proteins: Structure, Function and Bioinformatics, 2005, 60, 263-268.	2.6	29
97	Characterizing Changes in the Rate of Protein-Protein Dissociation upon Interface Mutation Using Hotspot Energy and Organization. PLoS Computational Biology, 2013, 9, e1003216.	3.2	29
98	Cyclophilic reactions of allene-1,3-dicarboxylic ester. Part 7. Synthesis of bicyclic and tricyclic heterocyclic compounds involving nitrogen, sulphur, and carbon as nucleophiles. Journal of the Chemical Society Perkin Transactions 1, 1988, , 2993.	0.9	28
99	Comparison of loop extrusion and diffusion capture as mitotic chromosome formation pathways in fission yeast. Nucleic Acids Research, 2021, 49, 1294-1312.	14.5	27
100	Model building by comparison at CASP3: Using expert knowledge and computer automation. Proteins: Structure, Function and Bioinformatics, 1999, 37, 47-54.	2.6	27
101	Predicting the Structure of Protein–Protein Complexes Using the SwarmDock Web Server. Methods in Molecular Biology, 2014, 1137, 181-197.	0.9	27
102	The preparation and dynamic behaviour of platinum(IV) derivatives of macrocyclic thioethers. Journal of Organometallic Chemistry, 1988, 341, 559-567.	1.8	26
103	Cost–benefit analysis of the mechanisms that enable migrating cells to sustain motility upon changes in matrix environments. Journal of the Royal Society Interface, 2015, 12, 20141355.	3.4	26
104	The structure of 2,2-dialkyl-1,3,2-oxathiastannolanes. Journal of Organometallic Chemistry, 1987, 325, 129-139.	1.8	25
105	A predicted three-dimensional structure for the human immunodeficiency virus binding domains of CD4 antigen. Protein Engineering, Design and Selection, 1989, 3, 13-21.	2.1	24
106	The preparation and characterisation of (disulphur dinitrido)bis(phosphine) complexes, [M(S2N2)(PR3)2](M = Pt, PR3= PMe3, PMe2PH, PMePh2, PPh3, PEt3, PPrn3, PBun3, or ½Ph2PCH2CH2PPh2; N Society Dalton Transactions, 1986, , 2367-2370.	⁄І) Ті ЕТQq 1:1	0 0 0 rgBT /
107	Cancer networks and beyond: Interpreting mutations using the human interactome and protein structure. Seminars in Cancer Biology, 2013, 23, 219-226.	9.6	23

108 Î²-diketone interactions. Journal of Molecular Structure, 1987, 161, 181-192.

3.6 22

#	Article	IF	CITATIONS
109	X-Ray structures of [Cu(cyclam)(H2O)2]F2·4H2O (cyclam = 1,4,8,11-tetra-azacyclotetradecane) and [Cu(en)2(H2O)2]F2·4H2O (en = ethylenediamine) reveal [F(H2O)4]–with strong hydrogen bonds. Journal of the Chemical Society Chemical Communications, 1988, , 1387-1388.	2.0	22
110	The syntheses, structures, and stereodynamics of [3]-ferrocenophane complexes III. Rhenium tricarbonyl halide complexes, fac-[ReX(CO)3(C5H4ECH3)2Fe] (X  Cl, Br, I; E  S, Se). Crystal structure of chloro-1,1′-bis(methylthio)ferrocenetricarbonylrhenium. Journal of Organometallic Chemistry, 1990, 383, 253-269.	1.8	22
111	383, 253-269 Plathum metal complexes of potentially chelating alkene thioether and selenoether ligands: the synthesis and dynamic nuclear magnetic resonance study of [MX2{E[(CH2)nCRCR2]2}](M = Pt or Pd; X =) Tj E cis-di-iodo-(5-thianona-1,8-diene)platinum(II), [PtI2{S[(CH2)2CHCH2]2}]. Journal of the Chemical Society	TQq1 1 0 1.1	.784314 rgt 21
112	The heteronuclear cluster chemistry of the Group 1B metals. Part 11. Effect of the nature of the bidentate diphosphine ligand on the metal framework structures of the gold heteronuclear cluster compounds [Au2Ru4(µ3-H)(µ-H){µ-Ph2P(CH2)nPPh2}(CO)12](n= 1–6). X-Ray crystal structures of [Au2Ru4(µ3-H)(µ-H){µ-Ph2P(CH2)nPPh2}(CO)12](n= 1 or 2). Journal of the Chemical Society Dalton	1.1	21
113	Transactions, 1989, , 1227-1236. Conformational analysis of the first observed non-proline cis-peptide bond occurring within the complementarity determining region (CDR) of an antibody. Journal of Molecular Biology, 1998, 284, 549-555.	4.2	21
114	A link between sequence conservation and domain motion within the AAA+ family. Journal of Structural Biology, 2004, 146, 189-204.	2.8	21
115	Emergence of novel cephalopod gene regulation and expression through large-scale genome reorganization. Nature Communications, 2022, 13, 2172.	12.8	21
116	The sticking point: how integrins bind to their ligands. Trends in Cell Biology, 1994, 4, 379-382.	7.9	20
117	Flexible Protein-Protein Docking with SwarmDock. Methods in Molecular Biology, 2018, 1764, 413-428.	0.9	20
118	Matrix feedback enables diverse higher-order patterning of the extracellular matrix. PLoS Computational Biology, 2019, 15, e1007251.	3.2	20
119	Structure and Function of Intercellular Adhesion Molecule-1. Chemical Immunology and Allergy, 1991, 50, 98-115.	1.7	19
120	Conversion of a phenylimido complex to a phenylamido complex by the potentially chelating ligand 2,3-dimethyl-2,3-butandiol(pinacol-H2): The crystal and molecular structures of [W2(NHPh)2(μ-pinacol)(pinacol)4] and the reaction side-product [W2(NPh)2(μ-O)(pinacol)2(pinacol-H)2]. Polyhedron, 1985, 4, 999-1005.	2.2	19
121	Polyhedron, 1985, 4, 999-1005 The neteronuclear cluster chemistry of the group 1B metals. Part 7. Synthesis and gold-197 MA¶ssbauer spectra of the mixed-metal cluster compounds [Au2Ru4(µ3-H)(µ-H){µ-Ph2E(CH2)nEâ€ ² Ph2}(CO)12](n= 1 or [Au2Ru4(µ3-H)(µ-H)(µ-Ph2AsCH2PPh2)(CO)12]. Journal of the Chemical Society Dalton Transactions,	2,) Tj ETÇ 1.1	0q1 1 0.7843 19
122	1900, , 1795 1801. The syntheses, structures and stereodynamics of transition metal complexes of 1,1′-bis(methylthio)ruthenocene. Crystal structure of 1,1′-bis(methylthio)ruthenocene tetracarbonyltungsten. Journal of Organometallic Chemistry, 1990, 394, 455-468.	1.8	19
123	Towards an automatic method of predicting protein stucture by homology: an evaluation of suboptimal sequence alignments. Protein Engineering, Design and Selection, 1992, 5, 305-311.	2.1	19
124	Developing a move-set for protein model refinement. Bioinformatics, 2006, 22, 1838-1845.	4.1	19
125	A Structural Systems Biology Approach for Quantifying the Systemic Consequences of Missense Mutations in Proteins. PLoS Computational Biology, 2012, 8, e1002738.	3.2	19
126	Fission yeast condensin contributes to interphase chromatin organization and prevents transcription-coupled DNA damage. Genome Biology, 2020, 21, 272.	8.8	19

#	Article	IF	CITATIONS
127	Halogenated Metabolites of the Red Alga Plocamium cruciferum. Australian Journal of Chemistry, 1979, 32, 2545.	0.9	18
128	Diaquabis(1,3-diaminopropane)copper(II) difluoride: X-ray structure reveals short hydrogen bonds between ligand waters and lattice fluorides. Inorganica Chimica Acta, 1988, 154, 17-20.	2.4	18
129	The heteronuclear cluster chemistry of the group 1B metals. Part 10. Synthesis, structures, and dynamic behaviour of the bimetallic hexanuclear group 1B metal cluster compounds [M2Ru4(µ3-H)2{µ-Ph2As(CH2)nEPh2}(CO)12](M = Cu or Ag; E = As or P; n= 1 or 2). X-Ray crystal structure of [Cu2Ru4(µ3-H)2{µ-Ph2As(CH2)2PPh2}(CO)12]. Journal of the Chemical Society Dalton Transactions,	1.1	18
130	A machine learning approach for ranking clusters of docked proteinâ€protein complexes by pairwise cluster comparison. Proteins: Structure, Function and Bioinformatics, 2017, 85, 528-543.	2.6	18
131	Comparative modelling: an essential methodology for protein structure prediction in the post-genomic era. Applied Bioinformatics, 2002, 1, 177-90.	1.6	18
132	The preparation and dynamic behaviour of platinum(IV) derivatives of macrocyclic sulphides; the X-ray crystal structure of fac-[PtMe3SCH2CH2SCH2CH2SCH2CH2]Cl·2H2O. Journal of the Chemical Society Chemical Communications, 1987, , 978-980.	2.0	17
133	Syntheses, electrochemistry, and spectroscopy of dirhodium(II) tetra-acetamidate and tetrakis(trifluoroacetamide) complexes with axial Group 15 substituents. The X-ray crystal structures of [Rh2(CH3CONH)4(AsPh3)2] and [Rh2(CH3CONH)4 –n(CH3CO2)n(MPh3)2], M = As or Sb, nâ‰^ 1. Journal the Chemical Society Dalton Transactions. 1989 581-588.	of ^{1.1}	17
134	Humanisation and characterisation of PR1A3, a monoclonal antibody specific for cell-bound carcinoembryonic antigen. Cancer Immunology, Immunotherapy, 1999, 47, 299-306.	4.2	17
135	Reactions of allene with triosmium and triruthenium clusters including coupling and oxidative addition: X-ray structure of the coupled allene compound [Os3(C6H8)(CO)10]. Journal of the Chemical Society Dalton Transactions, 1987, , 2935.	1.1	16
136	The hydrogen bonding of ligand fluoride: the X-ray crystal structure of difluoro(2,2′:6′,2″-terpyridine)copper(II) trihydrate. Inorganica Chimica Acta, 1988, 143, 25-29.	2.4	16
137	Stereochemical non-rigidity of dithioether complexes of trimethylplatinum(IV) halides. X-Ray crystal structures of [PtClMe3(MeSCH2CH2SEt)] and [PtIMe3(MeSCH2CH2SBut)]. Journal of the Chemical Society Dalton Transactions, 1988, , 521-531.	1.1	16
138	Structure of µ-fluoro-bis[bis(2,2′-bipyridyl)fluoronickel(II)] fluoride–ethanol (1/2) trihydrate, revealing several unique features including strong hydrogen bonds between fluoride ions and ethanol molecules. Journal of the Chemical Society Dalton Transactions, 1989, , 1273-1276.	1.1	16
139	Enhanced sampling of protein conformational states for dynamic crossâ€docking within the proteinâ€protein docking server SwarmDock. Proteins: Structure, Function and Bioinformatics, 2020, 88, 962-972.	2.6	16
140	Structure of tetraphenylphosphonium bis(benzenethiolato)aurate(I), [P(C6H5)4][Au(C6H5S)2]. Acta Crystallographica Section C: Crystal Structure Communications, 1985, 41, 862-865.	0.4	15
141	Aqua(2,2′-bipyridyl)difluorocopper(II) dihydrate: X-ray structure reveals short hydrogen bonds and other unusual features. Journal of the Chemical Society Dalton Transactions, 1987, , 2397-2399.	1.1	15
142	Synthesis, structure, and infrared spectroelectrochemistry of the cluster [Os3H(µ-FcCO)(CO)10](Fc =) Tj ETQqO the Chemical Society Chemical Communications, 1988, , 478-480.	0 0 rgBT 2.0	/Overlock 10 15
143	Platinum metal complexes of potentially chelating alkene–thioether and alkene–selenoether ligands: synthesis and dynamic nuclear magnetic resonance study of [MX2{MeE(CH2)nCHCH2}](M = Pt or Pd; X) Tj ET	Qq1 1 0.7 1.1	784314 rg8T 14
144	[PtBr2{{MeS(CH2)3CHi۠CH2}]. Journal of the Chemical Society Dalton Transactions, 1989, , 985-989. Alternating evolutionary pressure in a genetic algorithm facilitates protein model selection. BMC Structural Biology, 2008, 8, 34.	2.3	14

#	Article	IF	CITATIONS
145	Predicting improved protein conformations with a temporal deep recurrent neural network. PLoS ONE, 2018, 13, e0202652.	2.5	14
146	Structure of the dinuclear compound [Mo2(C5H5)2(CO)4(μ-Ph2PCH2PPh2)] in the crystal and in solution. Polyhedron, 1988, 7, 1793-1799.	2.2	13
147	Protonation versus oxidation in the reactions of trifluoroacetic acid with dinuclear osmium(I) complexes: molecular structure of [Os2(MeCo2)2(Âμ-H)(CO)4(PMe2Ph)2][PF6]. Journal of the Chemical Society Dalton Transactions, 1988, , 2753-2757.	1.1	13
148	The second domain of intercellular adhesion molecule-1 (ICAM-1) maintains the structural integrity of the leucocyte function-associated antigen-1 (LFA-1) ligand-binding site in the first domain. Biochemical Journal, 2000, 351, 79-86.	3.7	13
149	The structural basis for enhancerâ€dependent assembly and activation of the AAA transcriptional activator NorR. Molecular Microbiology, 2015, 95, 17-30.	2.5	13
150	Refinement of proteinâ€protein complexes in contact map space with metadynamics simulations. Proteins: Structure, Function and Bioinformatics, 2019, 87, 12-22.	2.6	13
151	Toward Patient-Specific Prediction of Ablation Strategies for Atrial Fibrillation Using Deep Learning. Frontiers in Physiology, 2021, 12, 674106.	2.8	13
152	Control of the metal core geometries and dynamic behaviour of heteronuclear group 1b metal cluster compounds using bidentate phosphine ligands: X-ray crystal structures of [Au2Ru4(µ-H)(Aµ3-H)(µ-Ph2PCH2PPh2)(CO)12] and [Ag2Ru4(µ3-H)2(µ-Ph2PCH2PPh2)(CO)12]. Journal Chemical Society Chemical Communications, 1986, , 600-602.	of the 0	12
153	Mixed-valence linear-chain complexes: X-ray structural characterization of a PdII/PdIVBr2 chain and of three mixed-metal chains, [NiPt(en)4Cl2]4+, [PdPt(pn)4Cl2]4+ and [NiPt(pn)4Cl2]4+, all as perchlorate salts. Acta Crystallographica Section B: Structural Science, 1989, 45, 147-152.	1.8	12
154	Cationic but-2-yne complexes of tungsten(II). Preparation and spectral properties of [WI(CO)L(dppm)(η2-MeC2Me)][BF4] (L = neutral monodentate oxygen and sulphur donor ligands). Crystal structure of [WI(CO){SC(NH2)2}(dppm)-(η2-MeC2Me)][ClO4]. Journal of Organometallic Chemistry, 1989, 372, 263-272.	1.8	12
155	Model building by comparison: A combination of expert knowledge and computer automation. Proteins: Structure, Function and Bioinformatics, 1997, 29, 59-67.	2.6	12
156	Phenylimido ethoxo complexes of tungsten(VI): Crystal and molecular structure of dichloro-di-μ- ethoxotetraethoxobis(phenylimido)ditungsten(VI). Polyhedron, 1987, 6, 163-173.	2.2	10
157	Fluoride-water hydrogen bonding: X-ray structure of tris(ethylenediamine)zinc(II) fluoride dihydrate. Inorganica Chimica Acta, 1989, 165, 191-195.	2.4	10
158	Mechanism of Cohesin Loading onto Chromosomes: A Conformational Dynamics Study. Biophysical Journal, 2010, 99, 1212-1220.	0.5	10
159	Bis(dimethylarsino)sulphide (dmas) complexes of the trimethylplatinum halides: the synthesis and characterization of fac-[(PtXMe3)(dmas)2] and the binuclear [(PtXMe3)2(dmas)] (X = Cl, Br, I) complexes, the crystal and molecular structure of [(PtBrMe3)2(dmas)]. Journal of Organometallic Chemistry, 1987, 325, 261-269.	1.8	9
160	Trimethylplatenum(IV) complexes of the dimethyldithioarsinate(V) anion: Preparation and molecular structure of the dinuclear [(PtMe3)2(Me2AsS2)2] and its selective fission to mononuclear [PtMe3(Me2AsS2)L] (L = PPh3, PPh2Me, py) complexes. Polyhedron, 1988, 7, 1855-1859.	2.2	9
161	Reactions of 2-thiopyridone and related N-, S- and C-methylated derivatives with [Rh2Cl2(CO)4]: crystal and molecular structure of fac-[Rh(MeC5H3NS)3] containing 6-methyl-2-thiopyridonato ligands. Inorganica Chimica Acta, 1988, 142, 37-41.	2.4	9
162	Tris(ethylenediamine)zinc(II) fluoride dihydrate: X-ray structure reveals a strongly hydrogen bonded difluoride cluster, [F2(H2O)2]2?. Journal of the Chemical Society Chemical Communications, 1989, , 738.	2.0	9

#	Article	IF	CITATIONS
163	The second domain of intercellular adhesion molecule-1 (ICAM-1) maintains the structural integrity of the leucocyte function-associated antigen-1 (LFA-1) ligand-binding site in the first domain. Biochemical Journal, 2000, 351, 79.	3.7	9
164	Structural Context of Exons in Protein Domains: Implications for Protein Modelling and Design. Journal of Molecular Biology, 2003, 333, 1045-1059.	4.2	9
165	An unprecedented reaction of diethyl azodicarboxylate with imidazolium ylides. Journal of the Chemical Society Chemical Communications, 1986, , 1745.	2.0	7
166	Aquadifluoro(1,10-phenanthroline)copper(II) dihydrate: X-ray crystal structure reveals strong hydrogen bonds between ligand fluoride and lattice water molecules. Journal of Crystallographic and Spectroscopic Research, 1987, 17, 605-613.	0.2	7
167	The heteronuclear cluster chemistry of the Group 1B metals. Part 13. Synthesis and structural characterization of the bimetallic hexanuclear Group 1B metal cluster compounds [M2Ru4(µ-CO)3(CO)10(PPh3)2](M = Cu, Ag, or Au). X-Ray structure analyses of [M2Ru4(µ-CO)3(CO)10(PPh3)2](M = Cu or Ag). Journal of the Chemical Society Dalton Transactions,	1.1	7
168	Probability-based model of protein-protein interactions on biological timescales. Algorithms for Molecular Biology, 2006, 1, 25.	1.2	7
169	Bis(acetato)bis[4-(N-acetylamino)pyridine]aquacopper(II)–hydrogen fluoride–hydrate (1/2/2): X-ray structure reveals H2O·HF hydrogen bonded in the lattice. Journal of the Chemical Society Dalton Transactions, 1988, , 1493-1496.	1.1	6
170	Triosmium clusters containing ligands derived from tropone (cycloheptatrienone): molecular structure of an oxidative addition product [Os3H(µ3-C7H5O)(CO)9]. Journal of the Chemical Society Dalton Transactions, 1987, , 551-555.	1.1	5
171	Molybdenum-molybdenum quadruple bonds: An asymmetrically substituted dimer containing a single acetate bridge. Crystal and molecular structure of [Mo2Cl3(μ-OAc)(PMe3)3]·PhMe. Polyhedron, 1987, 6, 2111-2118.	2.2	5
172	Magnetic properties and structure of MDT (TCNQ)2. Synthetic Metals, 1988, 27, 327-332.	3.9	5
173	β-Diketone interactions. Journal of Molecular Structure, 1989, 196, 249-255.	3.6	5
174	Electron acceptor molecules: new, expedient synthesis of substituted 7,7,8,8-tetracyano-p-quinodimethane (TCNQ) derivatives and the X-ray crystal structure of 2,5-dibromo-TCNQ. Journal of the Chemical Society Perkin Transactions 1, 1992, , 611.	0.9	5
175	Dinitration studies of 2,4,5-tribromo-3,6-dimethylphenol: the formation of an acyloin rearrangement product. Tetrahedron Letters, 1981, 22, 2325-2328.	1.4	4
176	Ϊƒ-η2Transformation of an electron-rich thioarsenic heterocyclic ligand: X-ray crystal structure of [Mo(η2-AsSCH2CH2S)(CO)2(η-C5H5)]. Journal of the Chemical Society Chemical Communications, 1987, , 983-984.	2.0	3
177	RaTrav: a tool for calculating mean first-passage times on biochemical networks. BMC Systems Biology, 2013, 7, 130.	3.0	3
178	Relapse models for clear cell renal carcinoma. Lancet Oncology, The, 2015, 16, e376-e378.	10.7	3
179	Development of a Deep Learning Method to Predict Optimal Ablation Patterns for Atrial Fibrillation. , 2019, , .		3
180	Model building by comparison: A combination of expert knowledge and computer automation. Proteins: Structure, Function and Bioinformatics, 1997, 29, 59-67.	2.6	3

0

#	Article	IF	CITATIONS
181	Application of deep learning methods: From molecular modelling to patient classification. Experimental Cell Research, 2022, 418, 113278.	2.6	3
182	The rearrangement of some 2-substituted-4-bromo-2,5-dinitro-6-hydroxy-3,6-dimethylcyclohex-3-en-1-ones. Tetrahedron Letters, 1981, 22, 1279-1280.	1.4	2
183	Structure of debrisoquinium sulfate. Acta Crystallographica Section C: Crystal Structure Communications, 1993, 49, 300-303.	0.4	2
184	Mean first-passage time calculations: comparison of the deterministic Hill's algorithm with Monte Carlo simulations. European Physical Journal B, 2012, 85, 1.	1.5	2
185	Bridging the gaps: atomic simulation of macromolecular environment brings together protein docking, interaction kinetics and the crowding effects. BMC Bioinformatics, 2010, 11, .	2.6	1
186	Abstract LB-356: An siRNA screen identifies Rsk1 as a key modulator of lung cancer metastasis. , 2011, , .		1
187	A Guide for Protein–Protein Docking Using SwarmDock. Methods in Molecular Biology, 2020, 2165, 199-216.	0.9	1
188	Conducting salts of cyclic sulphonium cations with 7,7,8,8-tetracyano-p-quinodimethane (TCNQ): X-ray crystal structure of 1-methyl-1,4-dithianium TCNQ salt, (MDT)1 +(TCNQ)2 ?. Journal of the Chemical Society Chemical Communications, 1988, , 1441.	2.0	0
189	The protein folding problem and tertiary structure prediction. Trends in Biochemical Sciences, 1995, 20, 129-130.	7.5	0
190	Optimisation of a Molecular Dynamics Simulation of Chromosome Condensation. , 2016, , .		0
191	Extracellular matrix anisotropy in breast cancer invasion and metastasis. European Journal of Cancer, 2016, 61, S102.	2.8	0
192	Lymphoblasts Produce a Lysosomal Protease That Rapidly Degrades L-Asparaginase - Implications for Therapy in Childhood Acute Lymphoblastic Leukemia Blood, 2007, 110, 2791-2791.	1.4	0
193	Interations of the Plasmodium falciparum—Infected Erythrocyte with ICAM-1. , 1993, , 92-103.		0

194 Prediction of the three dimensional structure of activin. , 1995, , 214-216.